Band offsets in ITO/Ga 2 O 3 heterostructures

Article *in* Applied Surface Science · June 2017
DOI: 10.1016/j.apsusc.2017.05.262

CITATIONS
2

READS
71

7 authors, including:

Patrick Carey
University of Florida
9 PUBLICATIONS **19** CITATIONS
SEE PROFILE

Fan Ren
University of Florida
1,054 PUBLICATIONS **19,453** CITATIONS
SEE PROFILE

David C. Hays
University of Florida
63 PUBLICATIONS **503** CITATIONS
SEE PROFILE

Sang-Phil Jang
Catholic University of Korea
113 PUBLICATIONS **671** CITATIONS
SEE PROFILE

Applied Surface Science 422 (2017) 179–183

Contents lists available at ScienceDirect

Applied Surface Science

journal homepage: www.elsevier.com/locate/apsusc

Full Length Article

Band offsets in ITO/Ga_2O_3 heterostructures

Patrick H. Carey IV[a], F. Ren[a], David C. Hays[b], B.P Gila[b], S.J. Pearton[b,*], Soohwan Jang[c], Akito Kuramata[d,e]

[a] Department of Chemical Engineering, University of Florida, Gainesville FL 32611 USA, USA
[b] Department of Materials Science and Engineering, University of Florida, Gainesville FL 32611 USA
[c] Department of Chemical Engineering, Dankook University, Yongin 16890, Korea
[d] Tamura Corporation, Sayama, Saitama 350-1328, Japan
[e] Novel Crystal Technology, Inc., Sayama, Saitama 350-1328, Japan

ARTICLE INFO

Article history:
Received 6 March 2017
Accepted 31 May 2017
Available online 2 June 2017

Keyword:
Ga_2O_3

ABSTRACT

The valence band offsets in rf-sputtered Indium Tin Oxide (ITO)/single crystal β-Ga_2O_3 (ITO/Ga_2O_3) heterostructures were measured with X-Ray Photoelectron Spectroscopy using the Kraut method. The bandgaps of the component materials in the heterostructure were determined by Reflection Electron Energy Loss Spectroscopy as 4.6 eV for Ga_2O_3 and 3.5 eV for ITO. The valence band offset was determined to be -0.78 ± 0.30 eV, while the conduction band offset was determined to be -0.32 ± 0.13 eV. The ITO/Ga_2O_3 system has a nested gap (type I) alignment. The use of a thin layer of ITO between a metal and the Ga_2O_3 is an attractive approach for reducing contact resistance on Ga_2O_3-based power electronic devices and solar-blind photodetectors.

1. Introduction

The β-polytype of Ga_2O_3 is attracting much recent interest for its applications to sensors, high power electronics and solar blind UV photodetectors [1–15]. The bandgap of this material (4.6 eV) is larger than that of either GaN or SiC and therefore has a higher theoretical breakdown field (~8 MV cm^{-1}) [1,3]. Experimental values have already reached 3.8 MV cm^{-1} [5] because of rapid progress in achievement of high quality bulk single crystals and epitaxial layers with controlled *n*-type conductivities [1,3]. Ga_2O_3 has other desirable properties, including high radiation hardness, good transport properties, a bandgap suited to true solar-blindness [14,15] and the commercial availability of low defect density wafers of large area. The promising device results for Ga_2O_3-based power rectifiers, transistors and solar blind photodetectors show that, given adequate thermal management methods, this material can expand the range of applications in military and commercial power switching and surveillance.

An issue with any new wide bandgap semiconductor technology is the need for low resistance improved Ohmic contacts that do not require excessive thermal treatments [16,17]. At this stage, only n-type Ga_2O_3 is available and so majority-carrier devices dominate. The lowest specific contact resistances achieved to date on Ga_2O_3 were in the range 4.6–8′10^{-6} Ω × cm^{-2} for Ti/Au contacts on n-Ga_2O_3 epitaxial layers in which Si ions were implanted and annealed at 925 °C to locally increase the doping concentration in the contact region [16]. This process was followed by dry etching, metal deposition and annealing at 470 °C [16]. Oshima et al. [17] reported use of sputtered Indium Tin Oxide (ITO) on n-Ga_2O_3, followed by annealing at 900–1150 °C. They found that Pt/ITO contacts on n-Ga_2O_3 showed superior Ohmic contacts to Pt/Ti and attributed this to the formation of an interfacial layer with lower bandgap and higher doping concentration than the Ga_2O_3 alone [17]. This interfacial layer promoted improved electron transport across the heterointerface

This is a case of one of the common approaches to lowering Ohmic contact resistance on wide bandgap oxide or nitride semiconductors, which generally take the form of surface cleaning or doping to reduce barrier height or increase of carrier concentration of the surface through preferential loss of oxygen (nitrogen) [3,6,7,18,19]. It is clear from the literature on Ga_2O_3 photodetectors that the current-voltage (I-V) characteristics for contacts on n-type Ga_2O_3 are not linear at low current and show the need for improved contact approaches. The large electron affinity of β-Ga_2O_3 (4.00 ± 0.05 eV) [19] means that there are few choices for making a direct Ohmic contact and interfacial layers will be needed. It is important to understand the band alignment at these heterointerfaces [20,21].

* Corresponding author.
E-mail address: spear@mse.ufl.edu (S.J. Pearton).

http://dx.doi.org/10.1016/j.apsusc.2017.05.262
0169-4332/

ITO is already commonly used a transparent current-spreading electrode on GaN-based light-emitting diodes [22] and is valued for its excellent electrical and optical properties and the fact its processing temperatures are compatible with standard semiconductor processes [23–29]. ITO-based transparent electrodes are standard in liquid crystal displays and it has a very low resistivity ($\leq 10^{-4}$ Ω.cm) due to the high carrier concentration ($>10^{21}$ cm^{-3}) and mobility (>50 cm^2/Vs) possible in this material [27,28][223,27,28]. To be used as a contact layer on Ga_2O_3, we need to establish the band alignment to ensure that there is no barrier to electron transport from the contact layer into the Ga_2O_3.

In this paper, we report on the determination of the band alignment in the ITO/Ga_2O_3 heterostructure. We employ X-Ray Photoelectron Spectroscopy (XPS) to determine the valence band offsets and by measuring the respective bandgaps of the ITO (3.5 eV) and Ga_2O_3 (4.6 eV), we were also able to determine the conduction band offset in ITO/Ga_2O_3 heterostructures.

2. Experimental

The ITO was deposited by RF magnetron sputtering on Ga_2O_3 and quartz substrates at room temperature using a 3-in. diameter target of pure ITO. The RF power was 125 W and the working pressure was 5 mTorr in a pure Ar ambient. The dc bias on the electrode under these conditions is in the range 30–40 V. The bulk β-phase Ga_2O_3 single crystals with (−201) surface orientation (Tamura Corporation, Japan) were grown by the edge-defined film-fed growth method. Hall effect measurements showed the sample was unintentionally n-type with an electron concentration of $\sim 3 \times 10^{17}$ cm^{-3}. Note that the samples were not exposed to air prior to the subsequent X-Ray Photoelectron Spectroscopy (XPS) measurements to avoid complications from surface contamination [30–35]. The latter may lead to less accurate band gap measurements when using reflection electron energy loss spectroscopy [36–38].

To obtain the valence band offsets, XPS survey scans were performed to determine the chemical state of the ITO and Ga_2O_3 and identify peaks for high resolution analysis [32,33]. A Physical Electronics PHI 5100 XPS with an aluminum x-ray source (energy 1486.6 eV) with source power 300W was used, with an analysis area of 2 mm × 0.8 mm, a take-off angle of 50° and an acceptance angle of ±7 degrees. The electron pass energy was 23.5 eV for the high resolution scans and 187.5 eV for the survey scans. The approximate escape depth (3 λ sin θ) of the electrons was 80 Å. All of the peaks are well-defined in this system and we didn't need to curve fit the data.

Charge compensation was performed using an electron flood gun, due to the dielectric nature of the films. The charge compensation flood gun is often not sufficient at eliminating all surface charge, and additional corrections must be performed. Using the known position of the adventitious carbon (C—C) line in the C 1 s spectra at 284.8 eV, charge correction was performed. During the measurements, all the samples and electron analyzers were electrically grounded so they were performed providing a common reference Fermi level. Differential charging can be a serious concern for photoemission dielectric/semiconductor band offset measurements [35]. While the use of an electron flood gun does not guarantee that differential charging is not present and in some cases could make the problem worse, our experience with oxides on conducting substrates has been that the differential charging is minimized with the use of an electron gun. Calibrations with and without the gun and verified that was the case. Our procedure has been described in detail previously [30,31]. In our experiments, we have not observed clear signs of differential charging between the ITO and the Ga_2O_3, but that does not preclude this effect being

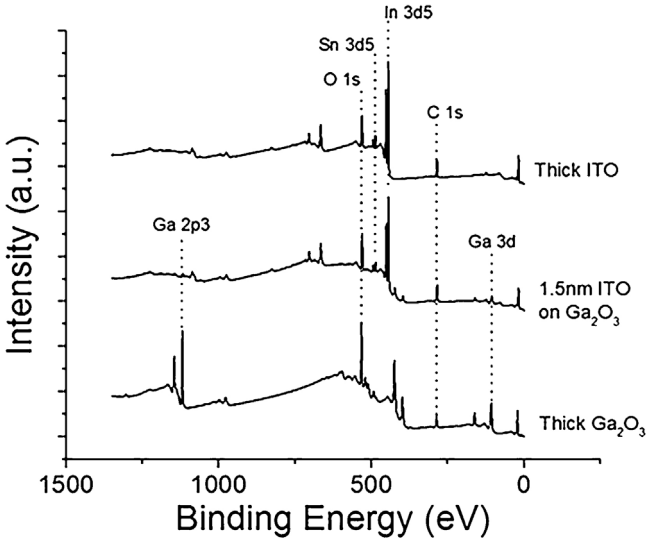

Fig. 1. XPS survey scans of ITO, 1.5 nm ITO on Ga_2O_3 and Ga_2O_3 bulk sample.

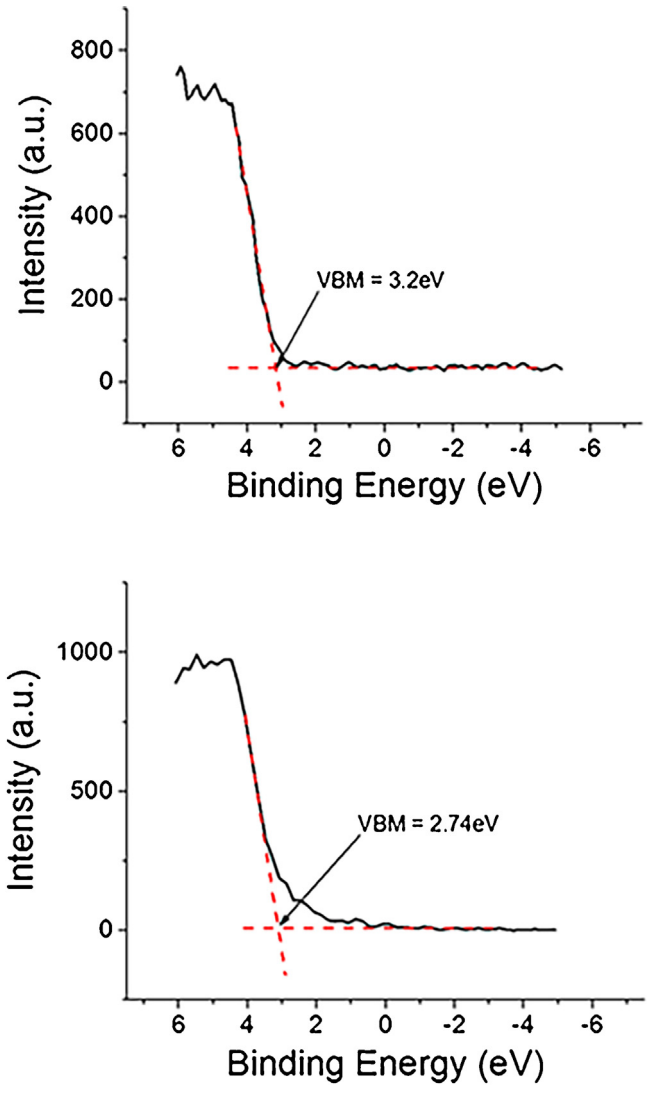

Fig. 2. XPS spectra of core levels to valence band maximum (VBM) for bulk Ga_2O_3 (top) and thick film ITO (bottom).

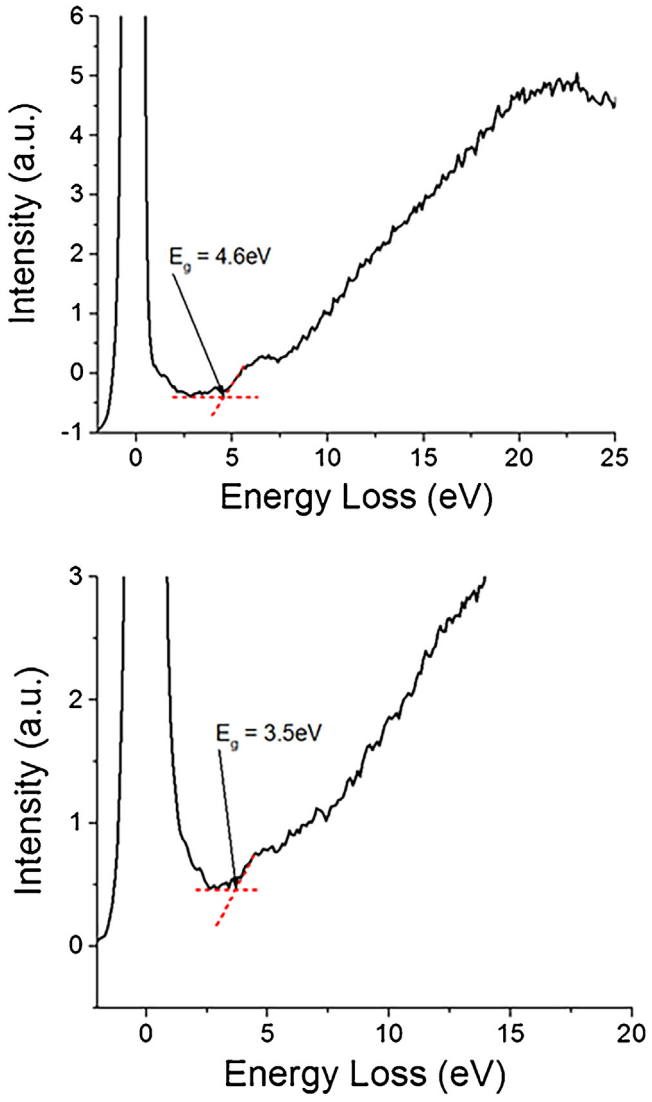

Fig. 3. Reflection electron energy loss spectra to determine the bandgap of bulk Ga_2O_3 (top) and for thick ITO (bottom).

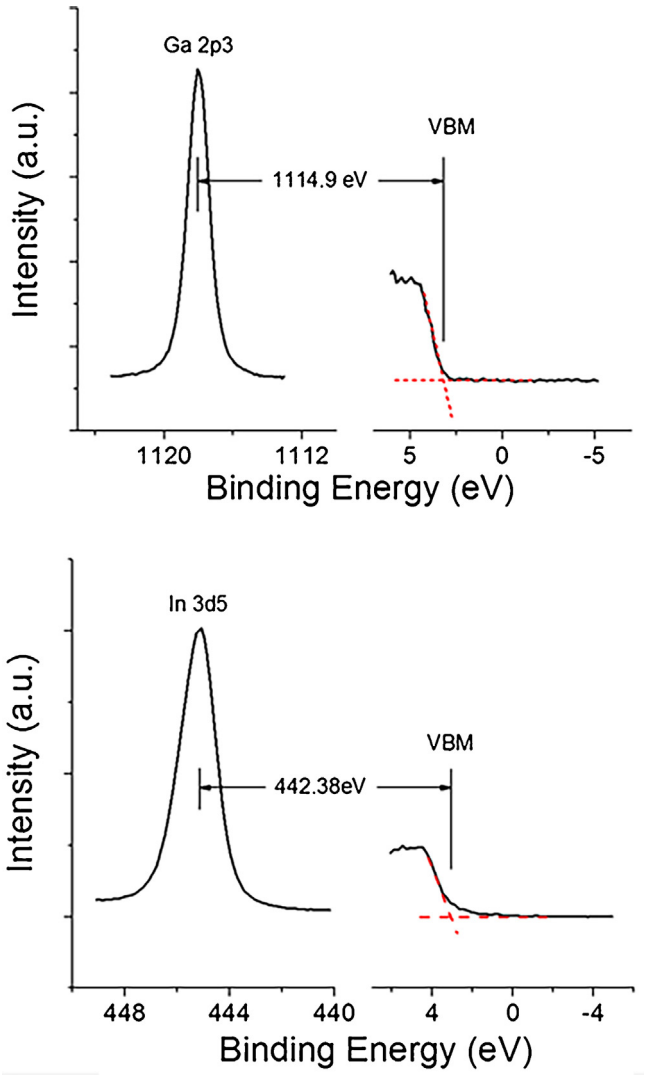

Fig. 4. High resolution XPS spectra for the vacuum-core delta regions of (top) the bulk Ga_2O_3 (top) and ITO (bottom).

present in future investigations of other oxides or different relative thicknesses of oxide and semiconductor or different conductivity levels in the Ga_2O_3.

Reflection electron energy loss spectroscopy (REELS) was employed to measure the bandgaps of the ITO and Ga_2O_3. REELS is a surface sensitive technique capable of analyzing electronic and optical properties of ultrathin gate oxide materials because the low-energy-loss region reflects the valence and conduction band structures [36–38]. While the UV/Vis technique requires relatively thick films (>0.5 μm) to determine the band gap, REELS has the advantage of only needing a thicker film than the sampling depth, so only a few nanometers are actually required. REELS spectra were obtained using a 1 kV electron beam and the hemispherical electron analyzer.

3. Results and discussion

Fig. 1 shows the XPS survey scans of thick (200 nm) ITO, 1.5 nm ITO on Ga_2O_3 and Ga_2O_3 bulk crystals. The spectra are free from contaminants and consistent with past published XPS data on these materials [20].

The valence band maximum (VBM) was determined by linearly fitting the leading edge of the valence band and the flat energy dis-

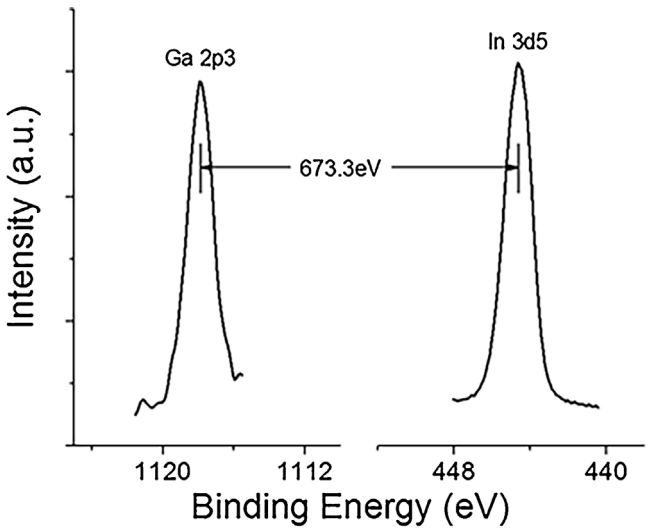

Fig. 5. High resolution XPS spectra for the Ga_2O_3 to ITO-core delta regions.

Table 1
Values of core levels and valence band offsets determined in these experiments (eV).

Reference Ga_2O_3				Reference ITO			Thin ITO on Ga_2O_3	
Ga_2O_3 metal core	Ga_2O_3 VBM	Metal Core level	Metal core-Ga_2O_3 VBM	ITO VBM	In 3d5 core-level	In 3d5-VBM	CL Ga 2p3-In 3d5	Valence band offset
Ga2p3	3.20	1118.10	1114.90	2.74	445.12	442.38	673.30	−0.78

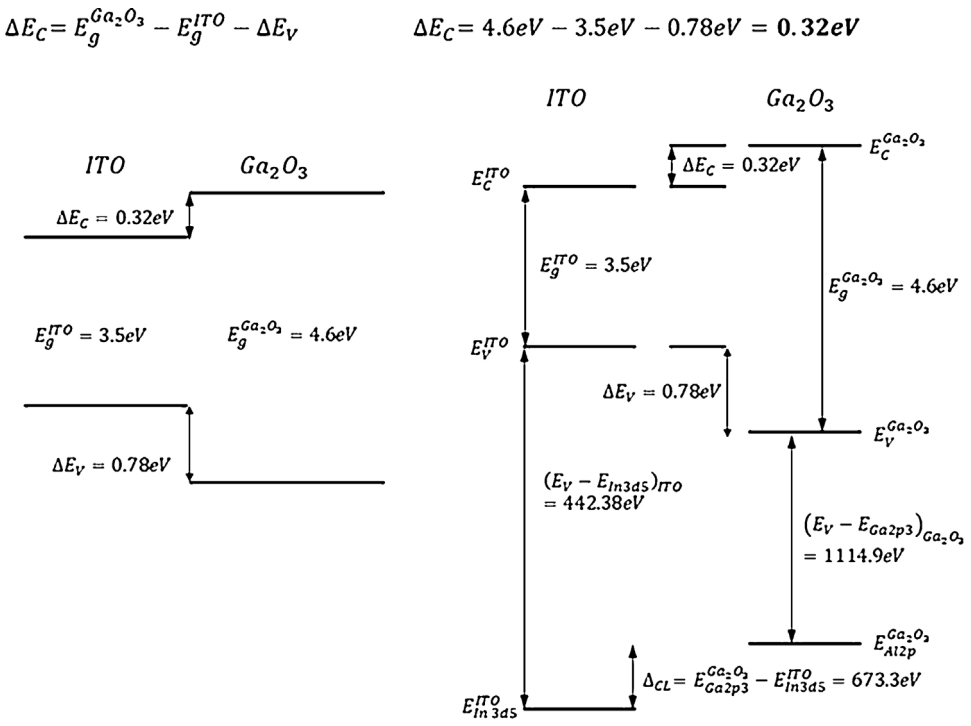

Fig. 6. Summary (left) and detailed (right) band diagrams for ITO/Ga_2O_3 heterostructure.

tribution from the XPS measurements, and finding the intersection of these two lines, as shown Fig. 2 for the bulk Ga_2O_3 (top) and thick ITO (bottom). The VBM was measured to be 3.2 ± 0.3 eV for Ga_2O_3, which is consistent with previous reports [20] and 2.74 ± 0.3 eV for the ITO.

The bandgap of the Ga_2O_3 was determined to be 4.6 ± 0.3 eV, as shown in the REELS spectra in Fig. 3 (top). The band gap was determined from the onset of the energy loss spectrum [36]. The measured band gap for the sputtered ITO was 3.5 ± 0.3 eV, which is consistent with literature values. The difference in bandgaps between ITO and Ga_2O_3 is therefore 1.1 eV and thus has the potential to provide a significant conduction band offset to enhance electron transport. To determine the actual band alignment and the respective valence and conduction band offsets, we examined the core level spectra for the samples.

High resolution XPS spectra of the VBM-core delta region are shown in Fig. 4 for the Ga_2O_3 (top) and thick ITO (bottom) samples. These were used to determine the selected core level peak positions. Fig. 5 shows the XPS spectra for the Ga_2O_3 to ITO-core delta regions of the heterostructure samples. These values are summarized in Table 1 for the three samples examined and these were then inserted into the following equation to calculate ΔEv [32,33]:

$$\Delta E_V = (E_{Core} - E_{VBM})_{Ref.Ga_2O_3} - (E_{Core} - E_{VBM})_{Ref.ITO} - \left(E_{Core}^{Ga_2O_3} - E_{Core}^{ITO}\right)_{Ga_2O_3}^{ITO}$$

Fig. 6 shows both a simplified and detailed band diagram of the ITO/Ga_2O_3 heterostructure. Our data shows this is a nested, type I alignment, with a valence band offset of 0.78 ± 0.21 eV and the conduction band offset is then 0.32 ± 0.1 eV using the following equation:

$$\Delta E_C = E_g^{Ga2O3} - E_g^{ITO} - \Delta E_V$$

ie. $\Delta E_C = 4.6eV - 3.5eV - 0.78eV = 0.32\,eV$

This data shows that in the as-deposited state, the ITO has a lower bandgap and favorable band alignment for improving electron transport across the heterointerface with n-type Ga_2O_3. Future work should investigate the effect of post-deposition annealing on the band alignment, as Oshima et al. showed that this greatly improved Ohmic contact resistance. As we discussed earlier, in these experiments we have found that charging and differential charging are not significant problems with the configuration and samples used. There are analytical methods for correction from the work by Bersch et al. [35] and physical methods to electrically isolate the entire sample, thereby eliminating the conductive film from gaining any lost electrons. If annealed samples are examined, such corrections might be needed if the conductivity of the materials near the surface changes significantly.

3.1. Summary and conclusions

The ITO/Ga_2O_3 heterojunction has a nested gap alignment of band offsets with a valence band offset of −0.78 eV and a conduction band offset of −0.32 eV determined from XPS measurements. The

insertion of ITO interlayers to improve contact resistance of Ohmic contacts on n-type Ga_2O_3 layers is an attractive option.

Acknowledgments

The project or effort depicted was also sponsored by the Department of the Defense, Defense Threat Reduction Agency, HDTRA1-17-1-011, monitored by Jacob Calkins. The content of the information does not necessarily reflect the position or the policy of the federal government, and no official endorsement should be inferred. The research at Dankook was supported by the Basic Science Research Program through the National Research Foundation of Korea (NRF) funded by the Ministry of Education (2015R1D1A1A01058663), and Nano Material Technology Development Program through the National Research Foundation of Korea (NRF) funded by the Ministry of Science, ICT and Future Planning (2015M3A7B7045185). Part of the work at Tamura was supported by "The research and development project for innovation technique of energy conservation" of the New Energy and Industrial Technology Development Organization (NEDO), Japan. We also thank Dr. Kohei Sasaki from Tamura Corporation for fruitful discussions.

References

[1] Masataka Higashiwaki, Kohei Sasaki, Hisashi Murakami, Yoshinao Kumagai, Akinori Koukitu, Akito Kuramata, Takekazu Masui, Shigenobu Yamakosh, Recent progress in Ga2O3 power devices, Semicond. Sci. Technol. 31 (2016), 034001-1–034001-12.
[2] M. Mohamed, C. Janowitz, R. Manzke, Z. Galazka, R. Uecker, R. Fornari, J.R. Weber, J.B. Varley, C.G. Van de Walle, The electronic structure of Ga2O3, Appl. Phys. Lett. 97 (2010), 211903-1–211903-1.
[3] M. Higashiwaki, K. Sasaki, A. Kuramata, T. Masui, S. Yamakoshi, Development of gallium oxide power devices, Phys. Stat. Solidi A 211 (2014) 21–25.
[4] Kelson D. Chabak, Neil Moser, Andrew J. Green, E. Walker Dennis Jr, E. Tetlak Stephen, Eric Heller, Antonio Crespo, Robert Fitch, Jonathan P. McCandless, Kevin Leedy, Michele Baldini, Gunter Wagner, Zbigniew Galazka, Xiuling Li, Gregg Jessen, Enhancement-mode Ga2O3 wrap-gate fin field-effect transistors on native (100) (-Ga2O3 substrate with high breakdown voltage, Appl. Phys. Lett. 109 (2016) 213501–213511.
[5] Andrew J. Green, Kelson D. Chabak, Eric R. Heller, Robert C. Fitch, Jr., Michele Baldini, Andreas Fiedler, Klaus Irmscher, Günter Wagner, Zbigniew Galazka, Stephen E. Tetlak, Antonio Crespo, Kevin Leedy, Gregg H. Jessen, 3.8-MV/cm breakdown strength of MOVPE-grown Sn-doped (-Ga2O3 MOSFETs, IEEE Electron, Dev. Lett 37 (2016) 902–906.
[6] M. Tadjer, N.A. Mahadik, V.D. Wheeler, E.R. Glaser, L. Ruppalt, A.D. Koehler, K.D. Hobart, C.R. Eddy, Jr., F.J. Kub, A (001) (-Ga2O3 MOSFET with a 2.9 V threshold voltage and HfO2 gate dielectric, ECS J. Solid State Sci.Technol. 5 (2016) 468–470.
[7] M.H. Wong, K. Sasaki, A. Kuramata, S. Yamakoshi, M. Higashiwaki, Field-plated Ga2O3 MOSFETs with a breakdown voltage of over 750 V, IEEE Electr. Dev. Lett. 37 (2016) 212–216.
[8] K. Sasaki, M. Higashiwaki, A. Kuramata, T. Masui, S. Yamakoshi, Ga2O3 Schottky barrier diodes fabricated by using single-crystal (–Ga2O3 (010) substrates, IEEE Electron. Dev. Lett. 34 (2013) 493–496.
[9] Man Hoi Wong, Kohei Sasaki, Akito Kuramata, Shigenobu Yamakoshi, Masataka Higashiwaki, Anomalous Fe diffusion in Si-ion-implanted (-Ga2O3 and its suppression in Ga2O3 transistor structures through highly resistive buffer layers, Appl. Phys. Lett. 106 (2015), 032105-1–032105-4.
[10] S. Oh, G. Yang, Jihyun Kim, Electrical characteristics of vertical Ni/(-Ga2O3 schottky barrier diodes at high temperatures, ECS J. Solid State Sci. Technol. 6 (2017) Q3022–Q3025.
[11] W.S. Hwang, A. Verma, H. Peelaers, V. Protasenko, S. Ruvimov, H. (Grace) Xing, A. Seabaugh, W. Haensch, C. Van de Walle, Z. Galazka, M. Albrecht, R. Fornari, D. Jena, High-voltage field effect transistors with wide-bandgap (-Ga2O3 nanomembranes, Appl. Phys. Lett. 104 (2014), 203111-1–203111-4.
[12] Shihyun Ahn, Fan Ren, Janghyuk Kim, Sooyeoun Oh, Jihyun Kim, Michael A. Mastro, S.J. Pearton, Effect of front and back gates on (-Ga2O3 nano-belt field-effect transistors, Appl. Phys. Lett. 109 (2016), 062102-1–062102-4.
[13] Janghyuk Kim, Sooyeoun Oh, Michael Mastro, Exfoliated Jihyun Kim, (-Ga2O3 nano-belt field-effect transistors for air-stable high power and high temperature electronics, Phys. Chem. Chem Phys. 18 (2016) 15760–15764.
[14] S. Oh, Y. Jung, M.A. Mastro, J.K. Hite, C.R. Kim, J. Eddy Jr, Development of solar-blind photodetectors based on Si-implanted (-Ga2O3, Opt. Exp. 23 (2015) 28300–28305.
[15] A.M. Armstrong, M.H. Crawford, A. Jayawardena, A. Ahyi, S. Dhar, Role of self-trapped holes in the photoconductive gain of (-gallium oxide Schottky diodes, J. Appl. Phys. 119 (2016), 103102-1–103102-5.
[16] K. Sasaki, M. Higashiwaki, A. Kuramata, T. Masui, S. Yamakoshi, Si-ion implantation doping in (-Ga2O3 and its application to fabrication of low-resistance ohmic contacts, Appl. Phys. Exp. 6 (2013), 086502-1–086502-4.
[17] T. Oshima, R. Wakabayashi, M. Hattori, A. Hashiguchi, N. Kawano, K. Saskai, T. Matsui, A. Kuramata, S. Yamakoshi, K. Yoshimatsu, A. Ohmoto, T. Oishi, M. Kasu, Formation of indium-tin-oxide ohmic contacts for (-Ga2O3, Jpn. J. Appl. Phys. 55 (2016), 1202B7-1–1202B7-3.
[18] E.G. Víllora, K. Shimamura, Y. Yoshikawa, T. Ujiie, K. Aoki, Electrical conductivity and lattice expansion of (-Ga2O3 below room temperature, Appl. Phys. Lett. 92 (2008) 202120.
[19] M. Mohamed, K. Irmscher, C. Janowitz, Z. Galazka, R. Manzke, R. Fornari, Schottky barrier height of Au on the transparent semiconducting oxide (-Ga2O3, Appl. Phys.Lett. 101 (2012), 132106-1–132106-4.
[20] Virginia D. Wheeler, David I. Shahin, Marko J. Tadjer, Charles R. Eddy Jr., Band alignments of atomic layer deposited ZrO2 and HfO2 high-k dielectrics with (-201) (-Ga2O3, ECS J. Solid State Sci. Technol. 6 (2017) Q3052.
[21] Z. Che, K. Nishhagi, X. Wang, K. Saito, T. Tanaka, M. Nishino, M. Arita, Q. Guo, Band alignment of Ga2O3/Si heterojunction measured by XPS, Appl. Phys. Lett. 109 (2016), 102106-1–102106-3.
[22] S.J. Kim, Improvement of gaN-based light-emitting-diode by indium tin oxide transparent electrode and vertical electrode, IEEE Photon. Technol. Lett. 17 (2005) 1617–1619.
[23] P.D.C. King, T.D. Veal, Present status and future prospects for development of non- or reduced- indium transparent conducting oxide thin films, J. Phys. C: Condensed Matter 23 (2011), 334214-1–334214-12.
[24] T. Minami, T. Miyata, Present status and future prospects for development of non- or reduced-indium transparent conducting oxide thin films, Thin Solid Films 517 (2008) 1474–1482.
[25] G.J. Exarhos, X.-D. Zhou, Discovery-based design of transparent conductig oxide films, Thin Solid Films 515 (2007) 7025–7052.
[26] Huiyong Liu, V. Avrutin, N. Izyumskaya, Ü. Özgür, H. Morkoç, Transparent conducting oxides for electrode applications in light-emitting and absorbing devices, Superlattices Microstruct. 48 (2010) 458–484.
[27] T. Minami, in: B.G. Svensson, S.J. Pearton, C. Jagadish (Eds.), Academic Press, San Diego, 2013;
Chapter 5 in Oxide Semiconductors, 88 of Semiconductors and Semimetals, ed.
[28] D. Ginley, H. Hosono, D.C. Paine, Handbook of Transparent Conductors, Springer, Berlin, Germany, 2011.
[29] A. Suzuki, T. Matsushita, T. Aoki, Y. Yoneyama, PLD of transparent conducting ITO films in magnetic field perpendicular to plume, Jpn. J. Appl. Phys. 40 (2001) L401–404.
[30] Hyun Cho, E.A. Douglas, A. Scheurmann, B.P. Gila, V. Craciun, E.S. Lambers, S.J. Pearton, F. Ren, Al2O3/InGaZnO4 heterojunction band offsets by X-Ray photoelectron spectroscopy, Electrochem. Solid-State Lett. 14 (2011) H431–434.
[31] D.C. Hays, B.P. Gila, S.J. Pearton, F. Ren, ZrSiOx/IGZO heterojunctions band offsets determined by X-ray photoelectron spectroscopy, Vacuum 122 (2015) 195–199.
[32] E.A. Kraut, R.W. Grant, J.R. Waldrop, S.P. Kowalczyk, Precise determination of the valence-band edge in X-Ray photoemission spectra: application to measurement of semiconductor interface potentials phys, Rev. Lett. 44 (1980) 1620–1625.
[33] E.A. Kraut, R.W. Grant, J.R. Waldrop, S.P. Kowalczyk, Semiconductor core level to valence-band maximum binding energy differences; precise determination by X-Ray photoelectron spectroscopy phys, Rev. B 28 (1983) 1965–1970.
[34] E.A. Kraut, Heterojunction band offsets and scaling, J. Vac. Sci. Technol. B 5 (1987) 1246–1252.
[35] E. Bersch, M. Di, S. Consiglio, R.D. Clark, G.J. Leusinkand, A.C. Diebold, Complete band offset characterization of the HfO2/SiO2/Si stack using charge corrected x-ray photoelectron spectroscopy, J. Appl. Phys. 107 (2010), 043702-1–043702-5.
[36] H.C. Shin, D. Tahir, S. Seo, Y.R. Denny, S.K. Oh, H.J. Kang, S. Heo, J.G. Chung, J.C. Lee, S. Tougaard, Reflection electron energy loss spectroscopy for ultrathin gate oxide materials, Surf. Interface Anal. 44 (2012) 623–627.
[37] J.C.H. Spence, Absorption spectroscopy with sub-anstrom beams: ELS in STEM, Rep. Prog. Phys. 69 (2006) 725–758.
[38] R.F. Egerton, Electron Energy Loss Spectroscopy in the Electron Microscope, Plenum, NY, 1996.